

Low Velocity Impact on Laminates Reinforced with Polyethylene and Aramidic Fibres

M.A.G. Silva & C. Cismaşiu

Centro de Investigação em Estruturas e Construção – UNIC, Faculdade de Ciências e Tecnologia, Universidade Nova de Lisboa, Quinta da Torre, 2829-516 Caparica, Portugal.

C.G. Chiorean

Faculty of Civil Engineering, Technical University of Cluj-Napoca, 15 C. Daicoviciu Str., 3400 Cluj-Napoca, Romania

ABSTRACT: The present study reports low velocity impact tests on composite laminate plates reinforced either with Kevlar 29 or Dyneema. The tests are produced using a Rosand Precision Impact tester. The experimental results obtained for Kevlar 29 are simulated numerically. The deflection history and the peak of the impact force are compared with experimental data and used to calibrate the numerical model.

1 INTRODUCTION

The intrinsic analytical difficulty of treatment of impact problems on composite laminates of polymeric matrix partially caused by the large number of parameters involved advises experimental testing to allow adequate certification of computational models that estimate the delamination, dynamic contact deformation, depth and area of damage, crashworthiness and correlated topics. Recent advances toward understanding damage mechanisms and mechanics of laminated composites (Abrate, 1998, Choi *et al.* 1992, Choi *et al.* 1991a,b, Fukuda *et al.* 1996), coupled with the development of advanced anisotropic material models (Clegg *et al.* 1999, Hayhurst *et al.*, 1999, Hiermaier *et al.*, 1999) offer the possibility of avoiding many experimental tests by using impact simulation. However, the numerical results should be used with precaution and must always be validated by experimental tests.

The present study reports low velocity impact, normal to the surface of laminated plates reinforced either with Kevlar 29 or with Dyneema, i.e. aramidic or tough polyethylene fibres. The paper concentrates essentially on macroscopic phenomenology and factors like stacking sequence, curing conditions, relative mass plate-impactor, stiffness or shape of striker are not examined. Calibration of the numerical model is described for the case of the Kevlar 29 plates.

All the simulations presented in the paper have been carried out by using the hydrocode AUTODYN (Autodyn, version 4.2), specially designed for non-linear transient dynamic events such as ballistic impact, penetration and blast problems. The software is based on explicit finite difference, finite volume and finite element techniques which use both grid based and gridless numerical methods. A new material model, specifically designed for the shock response of anisotropic material (Hayhurst *et al.*, 1999), has been implemented and couples non-linear anisotropic constitutive relations with a Mie-Grüneisen equation of state.

2 EXPERIMENTAL TESTS

Impact tests were performed using a Rosand Precision Impact Tester (Software manual, version 1.3), with a hemi-spherical headed striker indenting laminated plates at the centre of a circle of 100 mm diameter rigidly held by a steel ring. The experimental tests were conducted at INEGI Porto and the results reported in (Silva, 1999). Two sets of tests were considered, one on Kevlar 29 plates and the other on Dyneema plates.

The first set considered low speed impact on Kevlar 29 laminates. The plates were made from prepreg fabric impregnated with vinyl ester resin, at a curing temperature of 125°C, with eleven plies originating a thickness of 1.8mm.

The second set of tests corresponds to low speed impact on plates reinforced with high tenacity polyethylene fibres, Dyneema, pressed with eight plies, and a thickness of 1.7 mm and real density of 150g/m². The plates were pressed with a thermoplastic stamilex film with a melting temperature of 120°C. Averaged results indicated Young modulus E=3540MPa, failure stress σ_u =289MPa and strain at failure ϵ_u =5.6%. Thermoplastic matrices respond nonlinearly, cause higher damping and spread damage into larger regions than corresponding thermosetting matrices and are associated with significant damage on the tension face, even at low energies, and the strain on that face is believed to control damage initiation, but this property was less evident in tests, perhaps due to the ductility of the Dyneema matrix and its high toughness.

The results obtained for impact tests on Kevlar 29 and Dyneema plates with different impact energy are shown in Table 1.

Table 1. Characteristic values for impact on Kevlar 29 and Dyneema plates

Material	Dyneema			Kevlar 29		
	1	10	20	1	10	20
Nominal energy at impact (J)						
Maximum deflection (mm)	1.98	6.20	8.92	1.95	5.68	7.15
Deflection peak time (ms)	4.26	3.46	2.66	-	4.02	3.54
Maximum impact force (kN)	0.8	2.0	2.70	0.7	3.4	5.5
Force at peak time (ms)	-	-	-	-	3.10	2.68

Transmitted force is considerably higher for Kevlar 29 as energy level increases. The deflection peak time values appear with some delay with respect to Dyneema, material that exhibits higher damping.

3 NUMERICAL MODEL

The experimental tests obtained with Kevlar 29 are simulated numerically. In order to reduce the size of the problem, the numerical model contains only the head of the striker, modelled as a 5 mm radius steel sphere. Its density was adjusted as to ensure the same impacting mass as the one in the experimental tests. The target is modelled as a circular plate of 100 mm diameter and 1.8 mm thickness, firmly clamped on the edges. The relatively small diameter of the plate and the low velocity of the strikes make the boundary conditions extremely important and therefore must not be neglected.

The resulting model, see Figure 1, with two planes of symmetry, was obtained using the general purpose mesh generation program, TrueGrid (TrueGrid, version 2.1.0). The numerical analysis was performed taking advantage of axial symmetry. Both striker and target were modelled using the Lagrange processor, hexahedron brick elements, with 1.4 mm uniform cells size in the impact area.

In the Lagrangian mesh, the time step is automatically setup as to ensure that a disturbance does not propagate across a cell in a single time step.

As the solid Lagrange elements in AUTODYN have only one integration point at the centre of element they are sensitive to the hourglassing problem. These modes produce rigid body motion and the mesh starts self-straining, destroying the solution. In order to prevent this phenomenon, hourglass coefficient had to be increased to 0.15, the minimum value which prevents the generation of spurious modes.

4 MATERIAL PROPERTIES AND MODEL CALIBRATION

The most important characteristics and phenomena governing the behaviour of composite materials under ballistic impact are: material anisotropy, shock response, coupling of volumetric and deviatoric behaviour, anisotropic strength degradation, material compaction, phase changes. In

the case of anisotropic materials, there is a strong coupling between the equation of state and the constitutive relations, as volumetric strain leads to deviatoric stress and similarly, deviatoric strain leads to spherical stress. An advanced material model (Hayhurst *et al.*, 1999, Hiermaier *et al.*, 1999), specially designed to simulate the shock response of anisotropic materials, has recently been implemented as mentioned above, and couples the non-linear constitutive relations with the equation of state. The coupling is based on the methodology proposed by Anderson *et al.* (Anderson *et al.*, 1994). The model can additionally include compaction and orthotropic brittle failure criteria to detect directional failure such as delamination.

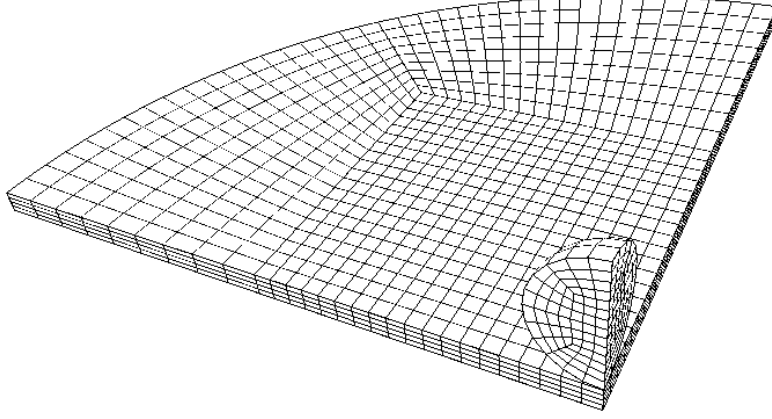


Figure 1. Numerical model

Composite materials of polymeric matrix subject to impact exhibit complex behaviour. Experimentally, the dominant tensile material failure modes were identified as extensive delamination, due to matrix cracking and/or matrix-fibre debonding, in-plane fibre failure and punching shear failure caused by a combination of delamination and fibre failure leading to bulk failure. In the numerical model the composite material is considered to be homogeneous. Kevlar fibres and matrix resin are not separately modelled and the main phenomena of relevance are accounted for in an macro-mechanical model.

Delamination is assumed to result from excessive through-thickness tensile stresses or strains and/or from excessive shear stresses or strains in the matrix material. In the incremental constitutive relation

$$\begin{Bmatrix} \Delta\sigma_{11} \\ \Delta\sigma_{22} \\ \Delta\sigma_{33} \\ \Delta\sigma_{23} \\ \Delta\sigma_{31} \\ \Delta\sigma_{12} \end{Bmatrix} = \begin{bmatrix} C_{11} & C_{12} & C_{13} & 0 & 0 & 0 \\ C_{21} & C_{22} & C_{23} & 0 & 0 & 0 \\ C_{31} & C_{32} & C_{33} & 0 & 0 & 0 \\ 0 & 0 & 0 & \alpha C_{44} & 0 & 0 \\ 0 & 0 & 0 & 0 & \alpha C_{55} & 0 \\ 0 & 0 & 0 & 0 & 0 & \alpha C_{66} \end{bmatrix} \begin{Bmatrix} \Delta\varepsilon_{11} \\ \Delta\varepsilon_{22} \\ \Delta\varepsilon_{33} \\ \Delta\varepsilon_{23} \\ \Delta\varepsilon_{31} \\ \Delta\varepsilon_{12} \end{Bmatrix} \quad (1)$$

the stress $\Delta\sigma_{11}$ normal to the laminate and the corresponding orthotropic stiffness coefficients C_{ij} are instantaneously set to zero, whenever the failure is initiated in either of those two modes, $j=1$ in equation(2):

$$\Delta\sigma_{ij} = 0 \text{ and } C_{ij} = C_{ji} = 0 \text{ for } i=1,3 \quad (2)$$

Delamination may also result from reduction in shear stiffness of the composite, via parameter α in equation (1). In-plane fibre failure is assumed to result from excessive stresses and/or strains in the 22 or 33 directions, $j=2$ or $j=3$ in equation (2). The combined effect of failure in all three material directions is represented changing the material stiffness and strength to isotropic characterisation, with no stress deviators or material tensile stresses. A fractional residual shear stiffness is maintained through the parameter α , whose value is obtained by experimental tests.

Composite material cell failure initiation criterion is assumed to be based on a combination of material stress and strain failure. Subsequent to failure initiation, the cell stiffness and strength properties are modified in agreement with the failure initiation modes.

The volumetric response of the material is defined through the solid equation of state. The polynomial sub-equation of state used in the numerical simulation, allows non-linear shock effects to be coupled with the orthotropic material stiffness.

All the reported tests were performed on Kevlar 29 composite target. The 4340 steel was represented using the Johnson-Cook strength model, which include strain and strain rate hardening and thermal softening effects. Material data for Kevlar 29 target and 4340 steel impactor are shown in Table 2.

The values characterising the orthotropic strength of the target were obtained in experimental tests carried out at Ernst-Mach-Institut in Germany. Quasi-static tensile tests were used to provide data on in-plane stiffness and failure strains. The through thickness stiffness was obtain in quasi-static compression tests. However, due to the fact that the sample thickness was less than 2 mm and because of instantaneous through thickness delamination, it was not possible to determine the Poisson's ratio, ν_{12} .

The value in the Table was derived iteratively through numerically low speed impact calibration. The calibration is based on the observation that the impact performance of target is dominated by the in-plane stiffness coefficients C_{22} and C_{33} in Equation 1. It can be shown (Tsai, 1988) that these coefficients depend on the in-plane and through thickness Young's moduli E_{22} and E_{11} and on Poisson's ratio ν_{12} and ν_{23} :

$$C_{22} = C_{33} = \frac{(1 - \nu_{12}\nu_{21})}{(1 + \nu_{23}) \cdot (1 - \nu_{23} - 2\nu_{21}\nu_{12})} E_{22}; \quad \nu_{21} = \frac{E_{22}}{E_{11}} \nu_{12} \quad (3)$$

Table 2. Material Data

KEVLAR 29	
Equation of states : <i>Orthotropic</i>	Tensile failure Stress 11 (kPa) $5.00E+04$
Sub-Equation of States : <i>Polynomial</i>	Maximum Shear Stress 12 (kPa) $1.00E+05$
Reference density (g/cm^3) 1.40	Tensile Failure Strain 11 0.01
Young modulus 11 (kPa) $2.392E+05$	Tensile Failure Strain 22 0.08
Young modulus 22 (kPa) $6.311E+06$	Tensile Failure Strain 33 0.08
Young modulus 33 (kPa) $6.311E+06$	Post Failure Response <i>Orthotropic</i>
Poissons ratio 12 0.115	Fail 11 & 11 Only
Poissons ratio 23 0.216	Fail 22 & 22 Only
Poissons ratio 31 3.034	Fail 33 & 33 Only
Strength : <i>Elastic</i>	Fail 12 & 12 and 11 Only
Shear modulus (kPa) $1.54E+06$	Fail 23 & 23 and 11 Only
Failure : <i>Material Stress/Strain</i>	Fail 31 & 31 and 11 Only
	Residual shear Stiff. Frac. 0.20
4340 Steel	
Equation of States : <i>Linear</i>	Yield Stress (kPa) $7.92E+05$
Reference density (g/cm^3) 7.83	Hardening constant (kPa) $5.10E+05$
Bulk modulus (kPa) $1.59E+07$	Hardening exponent 0.34
Reference temperature (K) 300	Strain rate constant 0.014
Specific heat capacity (J/kgK) 477	Thermal softening exponent 1.03
Strength : <i>Johnson-Cook</i>	Melting temperature (K) 1793
Shear modulus (kPa) $8.18E+07$	Failure model : <i>None</i>

On the other hand, the positiveness of the stiffness \mathbf{C} and the compliance $\mathbf{S}=\mathbf{C}^{-1}$ tensors in anisotropic materials is imposed by thermodynamic principles based on the fact that the elastic potential should remain always a positive quantity. The positive definiteness of these two tensors for the transversely isotropic materials implies that the following system of relations must hold (Jones, 1975):

$$|\nu_{12}| = |\nu_{13}| < \left(\frac{E_{11}}{E_{22}} \right)^{1/2}, \quad |\nu_{23}| < 1 \quad (4)$$

and

$$\nu_{12}^2 \nu_{23} < (1 - \nu_{23}^2) \frac{E_{11}}{2E_{22}} - \nu_{12}^2 \quad (5)$$

It can readily be derived from these relations in conjunction with the material data depicted in table 2, that the extreme positive limit of ν_{12} Poisson's ratio is $\nu_{12}^{\max} = 0.1219$.

The graph in Figure 2 illustrate the high sensitivity of the stiffness coefficient C_{22} for Poisson's ratio between 0.1 and $\nu_{12}^{\max} = 0.1219$. Therefore, the value of ν_{12} from Table 2 was obtained iteratively, equating the numerical response of the target with the experimental results.

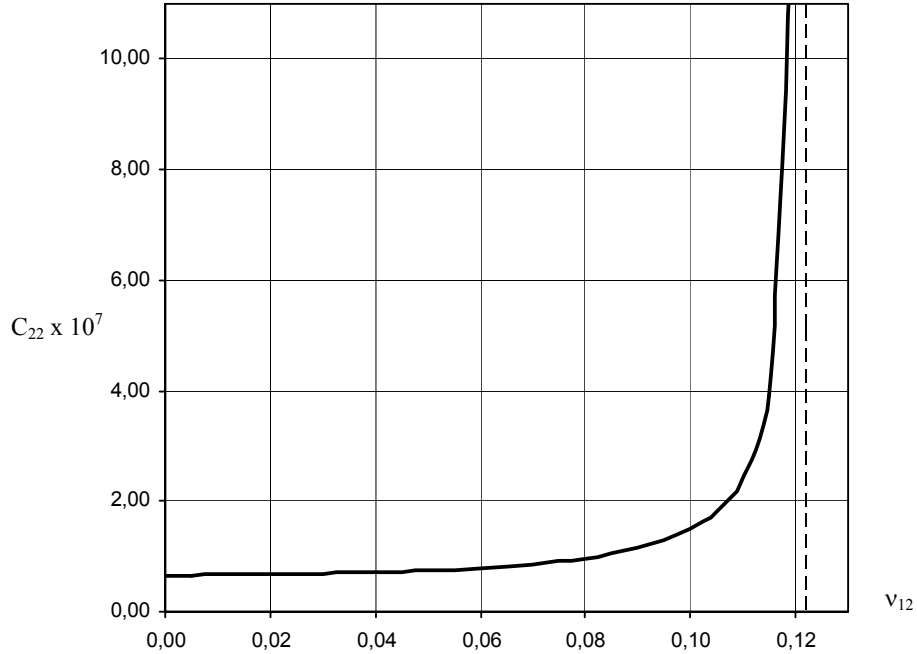


Figure 2. Variation of stiffness coefficient C_{22} with Poisson's ratio ν_{12}

5 COMPARISON OF RESULTS

The numerical estimates for the deflection history under the punch and the maximum impact force computed according to Hertz contact law (Hertz, 1982), were in good agreement with the experimental data for all energy levels, as shown in Figure 3. The numerical results predict a larger peak at an earlier stage than experimental tests. This trend is more evident for higher nominal impact energy. The increase of the peak value is clearly recognisable as is the earlier unloading with increase of the nominal energy at impact. The maximum deflection, δ_{\max} , and the corresponding peak time, t_p^δ , are shown in Table 3, for each energy level.

The maximum impact force, F_{max} , obtained for each level of nominal energy, and the corresponding peak time, t_p^F , are compared in Table 4, with the experimental values reported in (Silva, 1999).

Table 3. Maximum deflection and corresponding peak time

	Exp	Num	Exp	Num	Exp	Num	Exp	Num
Energy (J)	2		5		10		20	
δ_{max} (mm)	3.05	3.41	5.40	5.20	5.68	5.86	7.15	7.40
t_p^δ (ms)	4.96	5.01	5.14	4.74	4.02	3.85	3.54	3.68

Table 4. Maximum Impact Force and corresponding peak time

	Exp	Num	Exp	Num	Exp	Num	Exp	Num
Energy (J)	2		5		10		20	
F_{max} (kN)	1.10	1.25	1.70	1.78	3.50	3.40	5.50	5.60
t_p^F (ms)	4.12	3.80	3.84	3.92	3.10	2.70	2.68	2.40

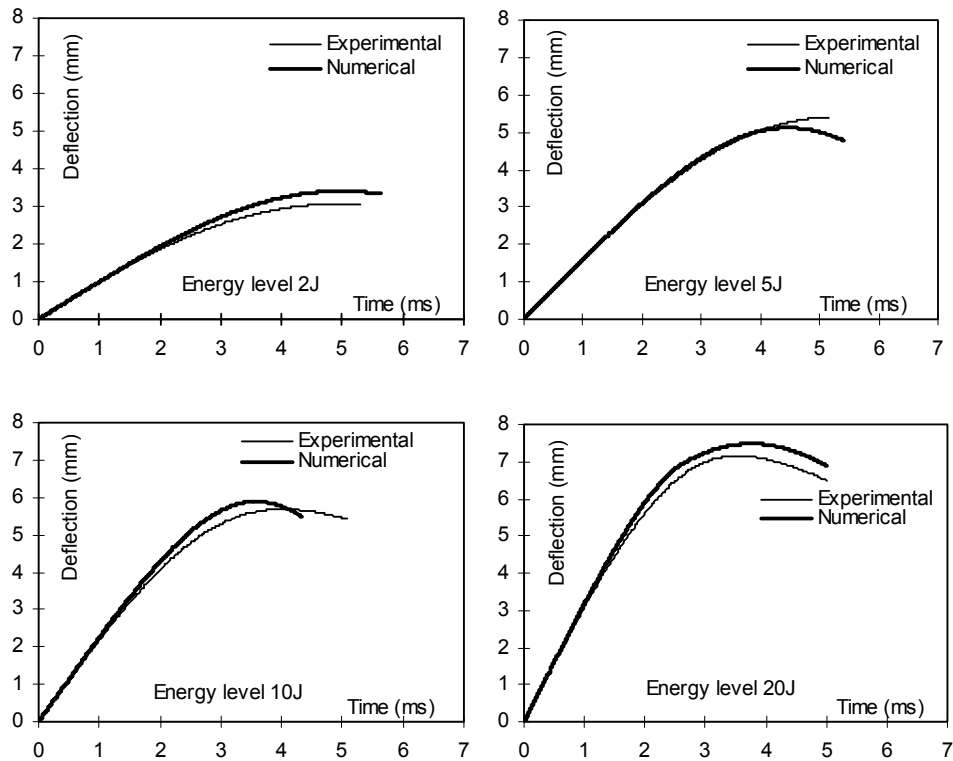


Figure 3. Deflection of the head of the striker

6 CONCLUSIONS

The experimental results show that laminates with lower bending stiffness allow higher *radiation damping*, reducing the impact forces, fact evidenced by Dyneema versus Kevlar. This effect is strengthened for laminates of lower mass which also exhibit lower contact force. Forces

transmitted by impactor reach maximum values earlier than the corresponding maximum deflection.

Energy dissipation in Dyneema plates is achieved through *plastic* deformation, whereas Kevlar plates deform more locally, facing delamination for higher forces.

Simulations of low speed impact on composite laminate plates reinforced with Kevlar 29 were performed using the finite difference numerical code AUTODYN-3D, based on an advanced mode for orthotropic materials (Hayhurst *et al.*, 1999). Its main draw is the ability to use a non-linear equation of state in conjunction with an orthotropic stiffness matrix which allows an accurate modelling of the response of composite materials under impact conditions.

The deflection history and the peak of the impact force are compared with experimental data, for four single strikes with energy levels of 2,5, 10 and 20J, respectively. The estimates for the displacements were in good agreement with the experimental data for all energy levels. The maximum relative error in the maximum displacement under the head of the striker, 11%, took place for the lowest energy level, 2J. The accuracy of the estimates increase with the energy level, as shown by a relative error of 2% for 20J. The peak of the impact force was computed according to the Hertzian contact model.

Compared with the experimental value, the relative error was 18% and 1.8% for the lowest and highest energy level, respectively. An explanation of these results could be the higher sensitivity of the numerical solutions to boundary conditions and hourglass effects in the case of low energy levels.

Future work is envisaged considering the numerical simulation of impact in Dyneema plates.

7 ACKNOWLEDGEMENT

This work is part of the research developed at DEC, Faculdade de Ciências e Tecnologia, supported by contract 43228/EME/2001 with Fundação para a Ciência e Tecnologia. Cooperation with colleagues from INEGI, Porto and Comd. F. Neto from Navy School of Lisbon is gratefully acknowledged.

8 REFERENCES

1. Abrate, S. 1998. *Impact on Composite Structures*. Cambridge University Press.
2. Choi, H.Y., Chang, F.K. 1992. A model for predicting damage in graphite/epoxy laminated composites resulting from low-velocity point impact. *Journal of Composite Materials*, 26(14):2134-2169.
3. Choi, H.Y., Downs, R.J., Chang F.K. 1991a. A new approach toward understanding damage mechanisms and mechanics of laminated composites due to low-velocity impact: Part I - Experiments. *Journal of Composite Materials*, 25:992-1011.
4. Choi, H.Y., Downs, R.J., Chang F.K. 1991b. A new approach toward understanding damage mechanisms and mechanics of laminated composites due to low-velocity impact: Part II - Analysis. *Journal of Composite Materials*, 25:1012-1038.
5. Fukuda, H., Katoh, F., Yasuda, J. 1996. Low velocity impact damage of carbon fiber reinforced thermoplastics. In *Progress in Durability Analysis of Composite Systems*, pages 139-145, Bakelma.
6. Clegg, R., Hayhurst, C.J., Leahy J., Deutekom, M. 1999. Application of coupled anisotropic material model to high velocity impact response of composite textile armour. In *18th Int. Symposium and Exhibition on Ballistics*, San Antonio, Texas USA, November 15-19.
7. Hayhurst, C.J., Hiermaier, S.J., Clegg, R.A., Riedel, W., Lambert, M. 1999. Development of material models for nextel and kevlar-epoxy for high pressures and strain rates. In *Hypervelocity Impact Symposium*, Huntsville, AL, Nov. 16-19.
8. Hiermaier, S.J., Riedel, W., Clegg, R.A., Hayhurst, C.J. 1999. Advanced material models for hypervelocity impact simulations. Technical report, ESA/ESTEC Contract No. 12400/97/NL/PA(SC).
9. Century Dynamics, Inc. *AUTODYN*. Interactive Non-Linear Dynamic Analysis Software, version 4.2, 1997.
10. *Rosand Precision Impact Tester*. Software Manual. Version 1.3.
11. Silva, M.A.G. 1999. Low speed impact on polyethylene and aramidic FRP laminates. In *Proceedings of Conference on Integrity, Reliability and Failure*, Porto, 19-22 July.
12. XYZ Scientific Applications, Inc. *TrueGrid*, version 2.1.0, 2000.

13. Anderson, C.E., Cox, P.A., Johnson, G.R., Maudlin, P.J.1994. A constitutive formulation for anisotropic materials suitable for wave propagation computer program. *Computational Mechanics*, 15:201-223.
14. Tsai, S.W. 1988.*Composite Design*, Think Composites, 4th edition
15. Hertz, O. 1882. Ueber die berührung fester elastischer körper. *Journal für die Reine und Angewandte Mathematik*, (92):156—171.
16. Jones, R.M. 1975. *Mechanics of composite materials*. Washington: Scripta Book Co.